IOP Conf. Series: Materials Science and Engineering **258** (2017) 012007 doi:10.1088/1757-899X/258/1/012007

Microstructure characterisation of Ti-6Al-4V from different additive manufacturing processes

M Neikter[1*], P Åkerfeldt[1], R Pederson[2] and M-L Antti[1]

[1] Division of Materials Science, Luleå University of Technology, Luleå 971 87, Sweden
[2] Division of Welding Technology, University West, Trollhättan 461 32, Sweden

* magnus.neikter@ltu.se, phone: +46 (0)920-492378

Abstract. The focus of this work has been microstructure characterisation of Ti-6Al-4V manufactured by five different additive manufacturing (AM) processes. The microstructure features being characterised are the prior β size, grain boundary α and α lath thickness. It was found that material manufactured with powder bed fusion processes has smaller prior β grains than the material from directed energy deposition processes. The AM processes with fast cooling rate render in thinner α laths and also thinner, and in some cases discontinuous, grain boundary α. Furthermore, it has been observed that material manufactured with the directed energy deposition processes has parallel bands, except for one condition when the parameters were changed, while the powder bed fusion processes do not have any parallel bands.

1. Introduction

Additive manufacturing (AM) has emerged as a promising manufacturing process for components with complex geometries and low lot sizes. Many different AM processes for metals have been developed [1-7], having different characteristics. Directed energy deposition processes where wire is used are preferred when higher deposition rates are wanted while powder bed fusion processes are better for manufacturing of parts with higher complexity. Titanium has high affinity to oxygen and if not protected in inert atmosphere during manufacturing, this will create a brittle surface layer beneath the metal surface called alpha case [8], which may significantly reduce important mechanical properties. The high oxygen affinity makes the production process of titanium sponge complex, which is one of the reasons why titanium metal is more expensive than e.g. steel. Furthermore, when taking into consideration manufacturing of components, titanium parts become even more expensive in the sense that up to 80% [9] of the original titanium material is machined away when using conventional subtractive manufacturing processes. Additive manufacturing is therefore extra attractive when considering making titanium alloy components. Additive manufacturing takes place in inert atmospheres, usually in argon gas or in vacuum. The loss of expensive titanium metal during AM is low for all processes. For powder bed fusion processes the powder that is not melted during the build can be recycled over and over again, making the final usage up to almost 100%, compared to conventional subtractive manufacturing with buy-to-fly ratios as low as 20% [9]. The typical microstructure of additive manufactured titanium consists of columnar prior beta (β) grains (see

section 3.1 for examples of prior β grains) that grow epitaxially [4,10-11] across several layers. When cooling below the β transus temperature alpha (α) phase starts to form, first at the β grain boundaries and then, depending on cooling rate, the α phase grows along the β grain boundaries or into the β grains in a platelet form (see figure 1 for examples of grain boundary α and α laths). The extent of alpha phase at the prior β grain boundaries as well as the size and distribution of α laths inside the prior β grains depend on cooling rate [2,6,12-14]. Faster cooling rates render in less or no alpha phase at the prior β grain boundaries, whereas the size (length/thickness) of individual α laths decreases with increasing cooling rate. Parallel band morphology is sometimes found in AM materials and could easily be interpreted as the deposited layers, which is not the case. As discussed by Kelly et al. [15] the parallel bands are rather a macroscopic phenomenon that is dependent on peak temperature, time at peak temperature and cooling rate. The aim of this work is to present typical microstructures and quantitative results of selected microstructure features that are characteristic for Ti-6Al-4V material built with the five chosen AM processes. It should be pointed out that significant variation of microstructures can be achieved within each AM process by varying the process parameters. As an example of that, Ti-6Al-4V material was built with Laser Metal wire Deposition (LMwD) using two different process parameter settings (LMwD-0 and LMwD-2).

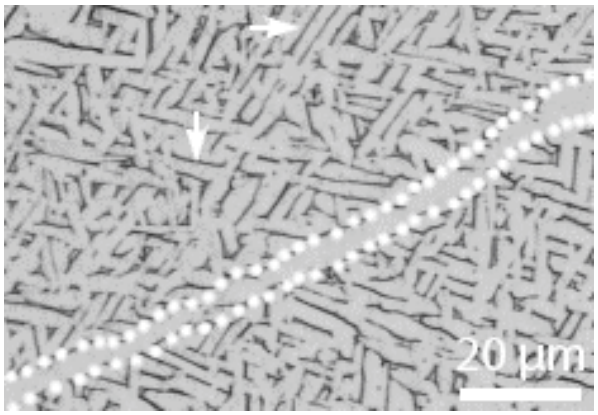

Figure 1. An example of a Ti-6Al-4V microstructure where the white dotted lines show the grain boundary α and the white arrows examples of α laths.

2. Method

In this work, the microstructure in material built from five different AM processes have been characterised, regarding the prior β grain size, α lath thickness and grain boundary α. The chosen AM processes for this investigation are LMwD, where a laser is used as energy source and a wire for deposition of material. Two differently built batches of material from this AM process have been investigated, one in which each layer was deposited continuously (LMwD-0) and one which included a two minutes break between each added layer (LMwD-2). Laser Metal powder Deposition (LMpD) is also investigated here, which is an AM process where laser combined with blown powder is used. TIG-torch energy source combined with wire is yet another process that has also been included in this work and it is here called Shaped Metal Deposition (SMD). These three AM processes (LMwD, LMpD and SMD) belong to the directed energy deposition group of AM processes. Two powder bed fusion processes were also investigated - Electron Beam Melting (EBM), where an electron beam is used as energy source, and Selective Laser Melting (SLM), where a laser beam energy source is used.
The SMD sample received a post heat treatment of 670 °C/2h, while the LMwD samples were exposed to 704 °C/2h. These heat treatments were performed for releasing stresses and do not affect the microstructure [16]. For the LMpD sample no post heat treatment was performed. The powder bed fusion materials were built using an EOS 290 machine (SLM) and an Arcam Q20 machine (EBM). None of the powder bed fusion materials where post build treated. In this work cross-sections perpendicular to the layers were characterised, i.e. cross sections across many layers. The sample

preparation was done according to conventional processes for titanium alloys. To reveal the microstructure, the samples were etched by Kroll's etchant consisting of 92 ml distilled water, 6 ml HNO_3 and 2 ml HF. The microstructure characterisation was done using a light optical microscope (LOM, Nikon Eclipse MA200) and its software (NIS Elements BR) and a stereomicroscope (Nikon SMZ1270).
The prior β grain measurements were performed in accordance to ASTM 112-13 [17] and by using large image stitching in the LOM. However, in order to measure the prior β grain size accurately, before each measurement the prior β grain boundaries were carefully marked in the images at a higher magnification by using an image editing software (Photoshop CC 2015), with stereomicroscope images taken into consideration. In total 500 prior β grain size measurements were done per sample.
The grain boundary α thickness was measured by using a grid tool in the LOM to avoid biased results and to obtain a more accurate average value of the thickness. A grid of squares (each square: 100x100 μm) was applied in the live image and within squares having grain boundary α one measurement was conducted. In total 200 measurements per sample were carried out.
The α laths were measured in five different areas on each sample; see illustrated location of the measurements in figure 2, denoted A-E in the EBM sample. In total 200 measurements per area were conducted, i.e. 1000 measurements per sample.

3. Results and discussion

3.1 Prior beta grains

In figure 2 macroscopic LOM overview images of Ti-6Al-4V material built with the five different AM processes are shown. Two characteristic prior β grains have been indicated with white dotted lines in the LMwD-0 and SLM materials. In Figure 3 the result of the prior β grain size measurements are summarized. Here it can be seen that material from the powder bed fusion processes (EBM and SLM) have smaller prior β grain size than the material built using directed energy deposition processes (LMwD, LMpD and SMD). This is clear also when comparing the materials of EBM and SLM with e.g. LMwD and SMD in Figure 2.
The prior β grain size is mainly determined by the time the material is exposed to temperatures above the β transus temperature. Normally the β transus temperature is around 995°C for Ti-6Al-4V, but the β transus temperature depends on the exact chemical composition of the alloy and can therefore vary between 970~1000°C [18]. Longer time and increased temperature above the β transus temperature lead to increased β grain size. Based on the findings in the present investigation it can be seen that the material built with the LMwD-0 and SMD processes have the largest prior β grains, whereas the materials from both powder bed fusion processes (EBM and SLM) show significantly smaller prior β grain size. It is thus evident that the materials built from LMwD-0 and SMD endure longer time above the β transus temperature compared to EBM and SLM. The reason for these differences are found in the different process setups (powder bed versus wire based deposition) and their distinct process parameters that influence the heat input. These differences then determine the cooling rate from above the β transus temperature and thus the prior β grain size.

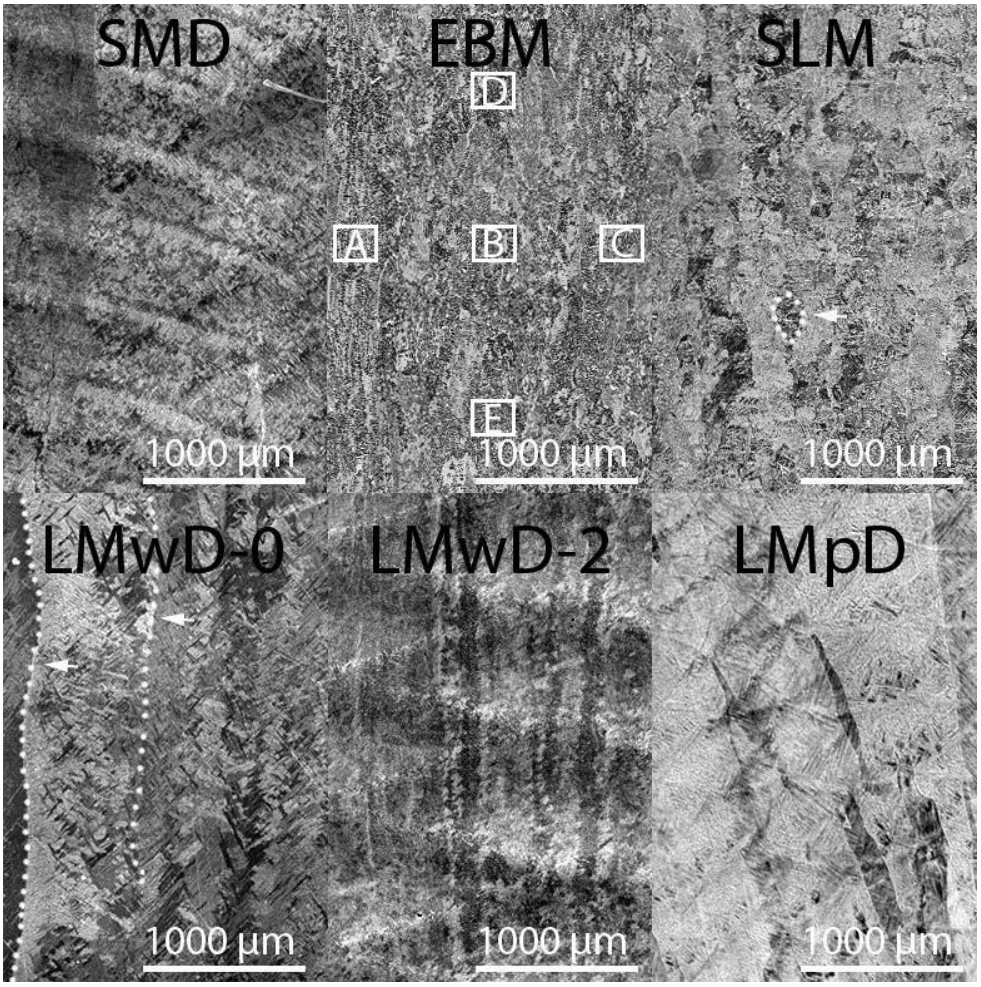

Figure 2. Overview LOM images of the different macrostructures of the five AM processes. The white arrows show prior β grain boundaries (white dotted lines) and the letters A-E illustrate the location of the α lath measurements on all the samples.

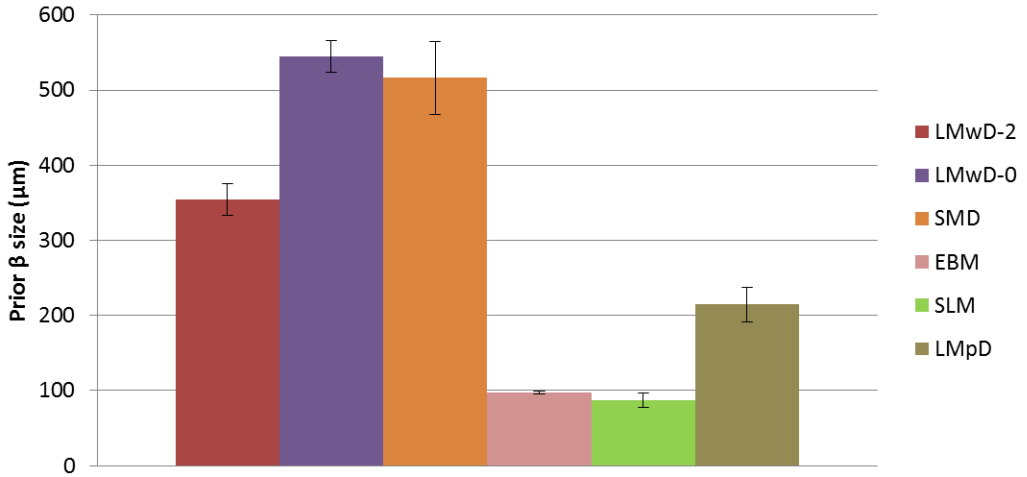

Figure 3. The prior β grain size in Ti-6Al-4V material built with five different AM processes. Overall the directed energy deposition based AM processes (LMwD, LMpD and SMD) have larger prior β grain sizes compared with material from the powder bed fusion processes (EBM and SLM).

3.2 Grain boundary alpha

The result of the grain boundary α measurements can be seen in Table **1**. The LMwD-0 material exhibits the thickest grain boundary α, followed by material from the powder bed fusion processes (EBM and SLM). Materials from LMwD-2 and SMD processes exhibit discontinuous grain boundary α with the average thickness less than one micrometer. Material from the LMpD process contains no grain boundary α and this is a result of the fast cooling of this AM process.

Table 1. Average and maximum thickness of grain boundary α in Ti-6Al-4V material built with different AM processes.

Name	Avg. grain boundary α	Max grain boundary α
LMwD-2	0.7 (discontinuous) ± 0.1	1.2
LMwD-0	3.5 ± 1.4	7.7
LMpD	-	-
SMD	0.6 (discontinuous) ± 0.1	1.0
EBM	2.9 ± 0.5	4.3
SLM	2.6 ± 0.7	4.6

3.3 Parallel bands

In Figure **2** parallel bands can be seen in the SMD, LMwD-2 and LMpD material. These are characterised by their wavy texture, which can be compared to e.g. EBM and SLM that have no parallel bands. Others have reported parallel bands for LMpD [13], LMwD [15] and SMD [4] as well. In the present work, the regions in between bands contain thicker α laths than regions within a band, where thinner α laths dominate. The reason for this is that the region with coarser α laths is closer to the fusion zone of next deposited layer, which renders in some coarseing of the microstructure closest to the fusion zone. This corresponds well with the findings of Sandgren et al. [2].

3.4 Alpha laths

Figure 4 shows overview LOM images of the different microstructures found in material from the investigated AM processes. The microstructure in material built using the LMpD process is unclear and difficult to distinguish, which suggests a martensitic transformed microstructure. The microstructures in the SMD and LMwD-2 material are very similar and are basket weave types of microstructures. The same type of microstructure, but coarser, is also found in the powder bed fusion manufactured materials, i.e. for EBM and SLM. The microstructure in the LMwD-0 material shows colonies of α laths, i.e. several α laths oriented in parallel forming colonies. This indicates that the cooling rate below the β transus temperature was slower than in materials built with the other AM processes, and the microstructure of LMwD-0 equates to the Widmanstätten colony morphology. In figure 4 the thicknesses of the laths are clearly visible, except for the LMpD material. The appearance of the α lath thicknesses is supported by the measurements shown in Figure 5 where SMD has the thinnest α laths with an average thickness of 0.7 μm, followed by LMwD-2 (1 μm), SLM (1.5 μm), EBM (1.5 μm) and LMwD-0 (2.3 μm). Seifi et al. [6] investigated EBM Ti-6Al-4V material and found the α laths to be in the range of 1 to 1.2 μm. Rafi et al. [14] investigated the α laths of SLM Ti-6Al-4V material and determined the thickness to be in the range of 1 to 2 μm. These results correspond well with the results in the present work.

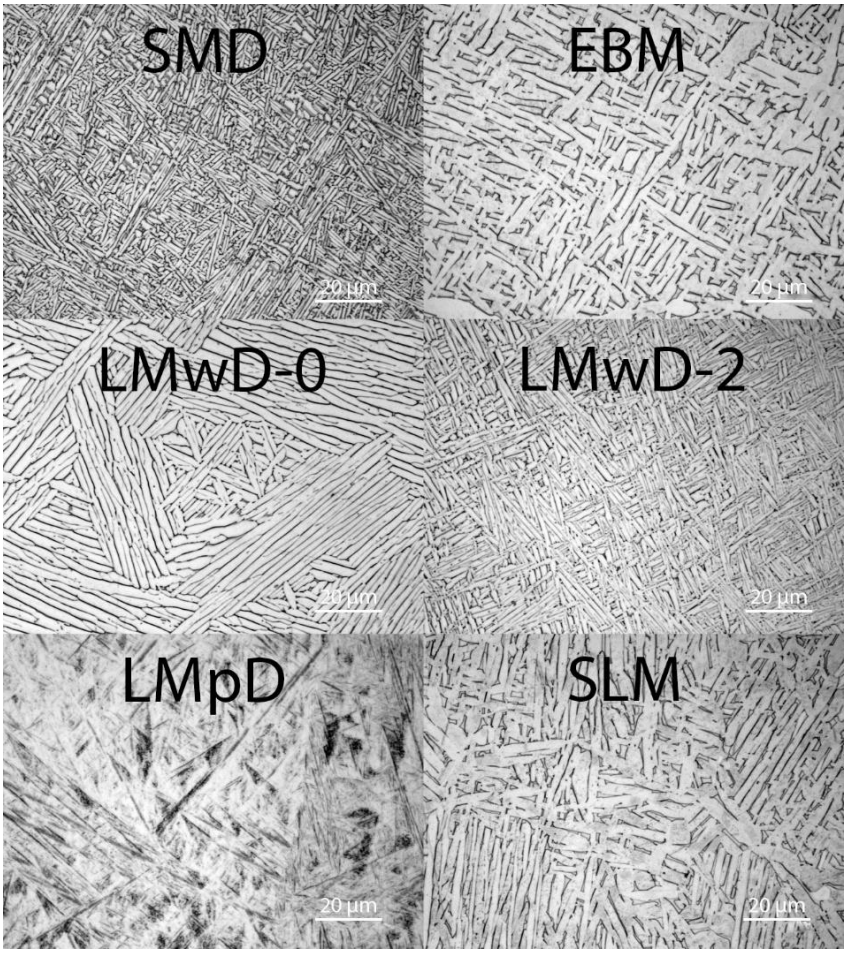

Figure 4. Overview of the different microstructures of the five AM- processes. SMD, EBM, LMwD-2 and SLM have basket weave morphology, LMwD-0 Widmanstätten colony and LMpD martensitic morphology.

Sandgren et al. [2] measured the α lath thickness to be 0.7 µm for their LMwD Ti-6Al-4V material, which corresponds well with the findings of Baufeld et al. [12], that found the corresponding thickness to be 0.6 µm. These results are close to the results found in the present work in the LMwD-2 Ti-6Al-4V material (1 µm). In order to investigate if the size of α laths varies in different regions of AM materials, different regions were selected within the same AM material, as depicted schematically in the micrograph for the EBM material in figure 2. The results from these measurements, shown in figure 5, reveal that in most types of AM material the α lath thickness is quite constant, even though the standard deviation for some of the materials is large, especially for the LMwD-0 material.
From the microstructural characterisation, it is possible to get an estimation of the mechanical properties of the different material. The α colony size is known to be the microstructural feature that is most important for the mechanical properties as it correlates with the slip length of the material [19]. Smaller α colonies render in higher strength and their size is somewhat correlating with the α lath and grain boundary α thickness, where the prior β grain set the boundary for how large the α colonies can become. Faster cooling rates decrease the size of the α colonies along with the thickness of the α laths and grain boundary α i.e. thinner α lath is closely linked to smaller α colonies. So, from the findings LMpD is estimated to have the highest strength of the here investigated material, while LMwD-0 is estimated to have the lowest.

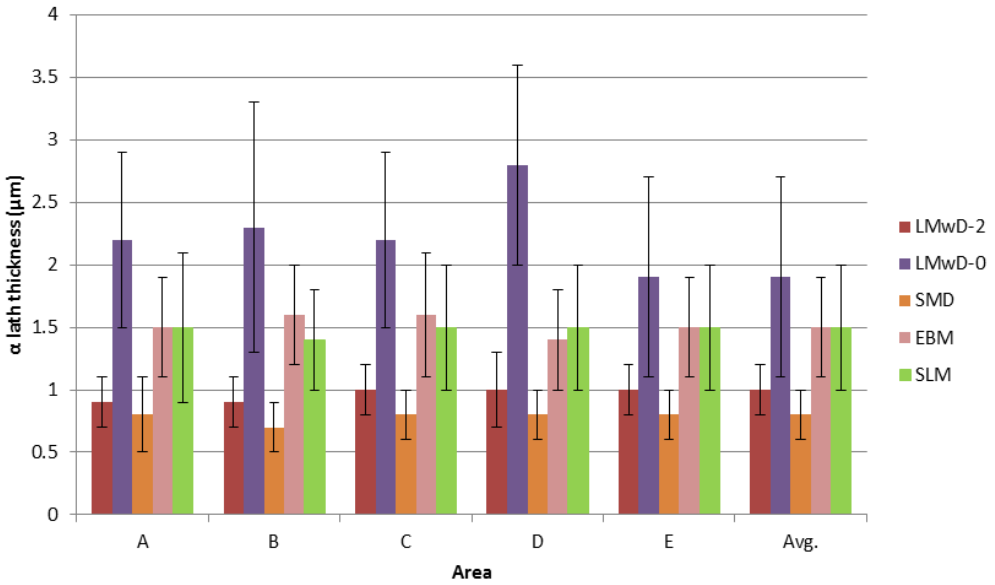

Figure 5. The α lath thickness in micrometer of the different AM processes on the different areas A-E, from figure 2. The column Avg. is the average of the five areas A-E.

The thickness of the grain boundary α along with the α colony size affect the ductility of the material, where very high cooling rates i.e. small α colonies and thin/non-existent grain boundary α render in poor ductility. Very slow cooling rates do not lead to the best ductility either, the ε_{max} is rather found at cooling rates of 100º C/min [19]. The cooling rates of the here investigated materials are above this rate which consequently results in that LMwD-0 is estimated to be the material with the highest ductility while LMpD should have the lowest. In between these two materials the mechanical properties of the other materials are most likely found by following the α lath thickness trend presented in this work.

4. Conclusions

In this work, materials manufactured with the powder bed fusion processes (EBM and SLM) have similar microstructures, i.e. prior β grain size, grain boundary α, and α lath size. The directed energy deposition processes (LMwD, LMpD and SMD) render in larger prior β grains than in material from the powder bed fusion processes. The parallel band phenomenon was present in materials from the SMD, LMpD and LMwD-2 processes, while non-existing in material from the LMwD-0, EBM and SLM built materials. Continuous manufacturing of Ti-6Al-4V material with the LMwD process, compared with introducing a 2 minutes holding time between each deposited layer, renders in significantly larger prior β grain size, thicker α phase layers in the prior β grain boundaries and thicker α laths.

Acknowledgements

The author would like to thank GKN Aerospace Engine Systems AB for their support throughout the project. Furthermore, the authors would also like to thank the student Viktor Sandell for his contributions.

References

[1] Śliwa R E, Bernaczek J and Budzik G 2016 The application of direct metal laser sintering (DMLS) of titanium alloy powder in fabricating components of aircraft structures *Key Engineering Materials* **687** pp 199-205

[2] Sandgren H R, Zhai Y, Lados D A, Shade P A, Schuren J C, Groeber M A, Kenesei P and Gavras A G 2016 Characterization of fatigue crack growth behavior in LENS fabricated Ti-6Al-

4V using high-energy synchrotron x-ray microtomography, *Additive Manufacturing A* **12** pp 132-41
[3] Mandil G, Le T T, Paris H and Suard M 2016 Building new entities from existing titanium part by electron beam melting: microstructures and mechanical properties *The International Journal of Advanced Manufacturing Technology* **85** pp 1835–46
[4] Baufeld B, van der Biest O and Gault R 2009 Microstructure of Ti-6Al-4V specimens produced by shaped metal deposition *International Journal of Material Research* **100** no. 11 pp 1536-42
[5] Al-Bermani S, Blackmore M L, Zhang W and Todd I 2010 The origin of microstructural, texture, and mechanical properties in electron beam melted Ti-6Al-4V *Metallurgical and Materials Transactions A* **41** pp 3422-34
[6] Seifi M, Salem A, Satko D, Shaffer J and Lewandowski J J 2016 Defect distribution and microstructure heterogeneity effects on fracture resistance and fatigue behavior of EBM Ti–6Al–4V *International Journal of Fatigue* **94** pp 263–87
[7] Sridharan N, Chaudhary A, Nandwana P and Babu S S, 2016, Texture evolution during laser direct metal deposition of Ti-6Al-4V *Journal of the Minerals, Metals & Materials Society* **68** no. 3 pp 772-7
[8] Sefer B, Roa J J, Mateo A, Pederson R and Antti M-L 2016 Evaluation of bulk and alpha-layer properties in Ti-6Al-4V at micro- and nano-metric length scale *Proc. of the 13th World Conference on Titanium* pp1619-24 DOI: 10.1002/9781119296126.ch271
[9] Gibson I, Rosen D and Stucker B 2010 *Additive Manufacturing Technologies: Rapid prototyping to direct digital manufacturing* p 246 Springer
[10] Formanoir C, Michotte S, Olivierrigo L G and Godet S, 2016, Electron beam melted Ti–6Al–4V: Microstructure,texture and mechanical behavior of the as-built and heat-treated material, *Materials Science & Engineering A* **652** pp 105–19
[11] Wang F, Williams S, Colegrove P and Antonysamy A A 2012 Microstructure and mechanical properties of wire and arc additive manufactured Ti-6Al-4V *Metallurgical and Materials Transactions A* **44** pp 968-77
[12] Baufeld B, Brandl E and Biesta O 2011 Wire based additive layer manufacturing: Comparison of microstructure and mechanical properties of Ti–6Al–4V components fabricated by laser-beam deposition and shaped metal deposition *Journal of Materials Processing Technology* **211** no. 6 pp 1146–58
[13] Zhai Y, Lados D A, Brown E J and Vigilante G N 2016 Fatigue crack growth behavior and microstructural mechanisms in Ti-6Al-4V manufactured by laser engineered net shaping *International Journal of Fatigue* **93** pp 51-63
[14] Rafi H, Karthik N, Gong H, Starr T L and Stucker B E 2013 Microstructures and mechanical properties of Ti6Al4V parts fabricated by selective laser melting and electron beam melting *Journal of Materials Engineering and Performance* **22** no. 12 pp 3872–83
[15] Kelly S and Kampe S 2004 Microstructural evolution in laser-deposited multilayer Ti-6Al-4V builds: Part I. microstructural characterization *Metallurgical and Materials Transactions A* **35** pp 1861-67
[16] Vrancken S, Thijs L, Kruth J and Van Humbeeck J 2012 Heat treatment of Ti6Al4V produced by Selective Laser Melting: Microstructure and mechanical properties *J.Alloys Compounds* **541** pp 177-85
[17] ASTM international *Standard test methods for determining average grain size* E112 – 13.
[18] Froes F H 2015 *Titanium Physical Metallurgy Processing and Applications* ASM International p 228
[19] Lütjering G 1998 Influence of processing on microstructure and mechanical properties of (α β) titanium alloys *Materials Science and Engineering: A* **243** no. 1 pp 32-45